THE JOURNAL OF PHYSICAL CHEMISTRY B

Article

pubs.acs.org/JPCB

# Light-Harvesting Polymers: Ultrafast Energy Transfer in Polystyrene-Based Arrays of π-Conjugated Chromophores

Zhuo Chen,[†,§] Erik M. Grumstrup,[‡,§] Alexander T. Gilligan,[‡] John M. Papanikolas,*[,‡] and Kirk S. Schanze*[,†]

[†]Department of Chemistry and Center for Macromolecular Science and Engineering, University of Florida, P.O. Box 117200, Gainesville, Florida 32611-7200, United States

[‡]Department of Chemistry, University of North Carolina at Chapel Hill, Chapel Hill, North Carolina 27599, United States

Supporting Information

**ABSTRACT:** Energy transfer along a nonconjugated polymer chain is studied with a polystyrene-based copolymer of oligo(phenylene-ethynylene) (OPE) donor and thiophene-benzothiadiazole (TBT) acceptor pendants. The graft copolymers are prepared from reversible addition−fragmentation transfer polymerization (RAFT) and copper(I)-catalyzed azide−alkyne "click" reaction. The singlet energy transfer from donor to accept is studied via fluorescence emission and ultrafast transient absorption spectroscopy. Near unity quenching of the OPE excited state by the TBT moiety occurs on multiple time scales (2−50 ps) dependent on where the initial exciton is formed on the polymer.

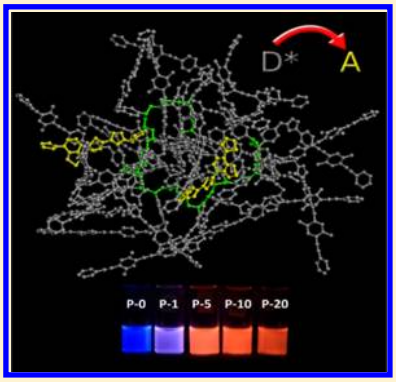


## INTRODUCTION

Multichromophoic light-harvesting macromolecules have been targeted for solar energy applications.[1−3] In conjugated polymers, such as poly(3-hexylthiophene) and polyfluorene, the backbone provides the light-harvesting function. Such materials can exhibit good processability, extraordinarily high extinction coefficients, and the ability to tune optical gaps and HOMO and LUMO energies. However, fully π-conjugated polymers are plagued by conformational disorder that breaks the chain into a series of segment chromophores with different conjugation lengths. This results in excited-state dynamics characterized by exciton self-trapping, exciton diffusion lengths that are limited to ∼10 nm, and low fluorescence quantum yields.[4−12] Alternative light-harvesting macromolecular architectures utilize polymers[1,13−19] or dendrimers[14,20−22] as scaffolds, bringing multiple pendant chromophores into close proximity while leaving their molecular electronic states intact.[23,24] With the development of controlled radical polymerization techniques, it is possible to prepare such polymers with well-defined chain structure and low polydispersity. Interchain and intrachain energy migration and energy transfer have recently been reported in polymers synthesized by controlled radical polymerization featuring a poly(methacrylate) backbone and oligo(phenylene ethynylene) (OPE) pendant chromophores.[25,26]

In the present Article we report the study of a series of light-harvesting polymers consisting of a well-defined nonconjugated polystyrene backbone functionalized with oligomeric π-conjugated chromophores. Energy transfer in these polychromophores is highly efficient, with dynamics and overall efficiency approaching that seen in fully π-conjugated polymers.[27] Femtosecond (fs) ultrafast time-resolved transient absorption spectroscopy is applied to study the dynamics of energy transfer in the polychromophores with high temporal resolution. While previous studies relying on fluorescence decay dynamics have provided qualitative insight regarding energy transfer dynamics in side-chain conjugated polymers,[25,26] the temporal resolution afforded here by femtosecond transient absorption considerably exceeds that which has been accomplished in previous work. The results of this study are unique because they provide clear insight regarding the dynamics of intrachain energy transfer within side-chain conjugated polymers.

## EXPERIMENTAL METHODS

**Materials and Synthesis.** All reagents were used as received unless otherwise specified. 4-Vinylbenzyl was passed through a short neutral alumina column to remove inhibitors prior to use. CuBr was purified by washing three times with glacial acetic acid and three times with absolute ethanol. Detailed synthetic procedures and structural characterization of polymers and compounds are provided in Supporting Information.

**Instrumentation and Methods.** NMR spectra were measured on a Gemini-300 FT-NMR, a Mercury-300 FT-NMR, or an Inova-500 FT-NMR. High resolution mass spectrometry was performed on a Bruker APEX II 4.7 T Fourier Transform Ion Cyclotron Resonance mass spectrometer (Bruker Daltonics,

Received: November 25, 2013
Published: December 3, 2013

   dx.doi.org/10.1021/jp411565p | J. Phys. Chem. B 2014, 118, 372−378

Billerica, MA). Gel permeation chromatography (GPC) analyses were carried out on a system composed of a Shimadzu LC-6D pump, an Agilent mixed-D column, and a Shimadzu SPD-20A photodiode array (PDA) detector, with THF as eluent at 1 mL/min flow rate. The system was calibrated against linear polystyrene standards in THF.

UV−visible absorption measurements were carried out on a Shimadzu UV-1800 dual beam absorption spectrophotometer using 1 cm quartz cells. Photoluminescence measurements were obtained on a fluorimeter from Photon Technology International (PTI) using 1 cm quartz cells. Photoluminescence lifetimes were obtained by time-correlated single photon counting (TCSPC) using a single photon counting Fluo Time 100 (Picoquant) Fluorescence Lifetime Spectrometer, and excitation was provided using a PDL 800-B Picosecond Pulsed Diode Laser (375 nm).

For transient absorption spectroscopy, samples were dissolved in THF to an OD of between 0.4 and 0.5 in a 2 mm cuvette. Femtosecond pulses were derived from a Clark-MXR CPA 2210 Ti:sapphire laser which produces ∼150 fs pulses centered at 775 nm with a 1 kHz repetition rate. A portion of the output was frequency doubled (to 388 nm) in a BBO crystal and used for photoexcitation of the donor. Low fluences (25 $\mu$J/cm$^2$) were necessary to achieve linear behavior of the transients. Kinetics were monitored by a weak continuum probe pulse generated by focusing a small portion of the 775 nm fundamental into a translating $CaF_2$ window. Spectra were collected at a rate of 1 kHz with pump on and pump off spectra interleaved by mechanical chopping, are chirp corrected for delay times $\Delta t < 20$ ps, and are each the average of 8000 individual pump on and pump off spectra.

The Förster radii were calculated from molar absorptivity of the acceptor and the corrected emission spectrum of the donor according to:

$$k = \frac{1}{\tau_D}\left(\frac{R_0}{r}\right)^6$$

$$R_0^6 = \frac{9000 \ln(10)\phi_D\langle K^2\rangle}{128\pi^5 n^4 N}\int_0^\infty \frac{\sigma_{fl}(\nu)\varepsilon_{(abs)}(\nu)}{\nu^4}d\nu$$

| | |
|---|---|
| $\tau_D$ | donor emission lifetime (1 ns) |
| $r$ | chromophore distance |
| $R_0$ | Förster distance |
| $\phi_D$ | donor quantum yield |
| $K$ | orientational factor (set to 0.667 for our calculation) |
| $n$ | index of refraction of THF 1.407 |
| $N$ | Avogadro's number |
| $\sigma_{fl}(\nu)$ | fluorescence spectrum of donor normalized to unit area |
| $\varepsilon_{(abs)}$ | molar extinction spectrum of acceptor |
| $(\nu)$ | in units of cm$^{-1}$ |

Molecular dynamics (MD) simulations were performed on 30 repeat unit polymers with 0, 2, 3, and 6 TBT chromophores placed randomly in the structure to represent the **P-0**, **P-5**, **P-10**, and **P-20** copolymers, respectively. Monomer repeat units with TBT and OPE chromophores were geometrically optimized with the B3LYP DFT functional and a 6-31G+ basis set as implemented in Gaussian09 version 09a02.[28] The structures and DFT-determined atomic charges were imported into the Materials Studio software package for MD. Unit cells consisting of the polymers along with explicit THF solvent were annealed with 10 temperature cycles ranging from 300 to 500 K using the Universal Force Field[29] as implemented in the Forcite module of Materials Studio. The final minimum of the annealing cycle was taken as the starting point for subsequent MD runs. MD on each of the four polymers showed the minimum distance between chromophores was independent of chromophore identity (i.e., TBT−OPE distance or OPE−OPE distance), so to boost statistical relevance of the dynamics runs, all neighboring OPE−OPE distances of the **P-0** polymer were tracked to find the minimum distance reported in the manuscript. Molecular dynamics were performed on two separate **P-0** polymers (last and penultimate energy minima of the annealing cycling). The first structure was run for a total of 20 ns. The second was run for 6 ns.

## RESULTS AND DISCUSSION

**Polymer Structures, Synthesis, and Characterization.** The structures of the polymers that are the focus of this investigation are shown in Chart 1. They feature an atactic polystyrene backbone functionalized with pendant $\pi$-conjugated chromophores. Two $\pi$-conjugated chromophores with distinct singlet excited-state energies were attached to the polystyrene scaffold. In particular, an oligo(phenylene-ethynylene) (OPE), which has a relatively high singlet energy (3.05 eV), serves as energy donor, whereas the thienyl-benzotriazole-thienyl (TBT) oligomer, with a lower singlet energy (2.07 eV), acts as energy acceptor. This pair of chromophores was selected because the fluorescence of the OPE donor and the absorption of the TBT acceptor overlap well to give rise to efficient singlet−singlet energy transfer. In addition, both chromophores have very high fluorescence quantum yields (>0.75) and their absorption spectra overlap minimally. The high fluorescence yields allow quantification of the energy transfer efficiency, and the distinct absorption profiles allow selective excitation of either chromophore in the polymers. In essence, the properties of the two chromophores are nearly ideal for the quantitative study of intrapolymer energy transfer efficiency and dynamics. A series of five polychromophores with different OPE/TBT ratios were prepared (**P-*x***) where ***x*** represents the percentage of TBT groups in the polymer (Chart 1).

The synthetic route to prepare the five polychromophores with different OPE/TBT ratios (**P-*x***, where ***x*** represents the percentage of TBT groups in the polymer) are shown in Scheme 1;

**Chart 1. Structures of Polymers (P-0 to P-20) and Model Compounds (1a and 1b)**

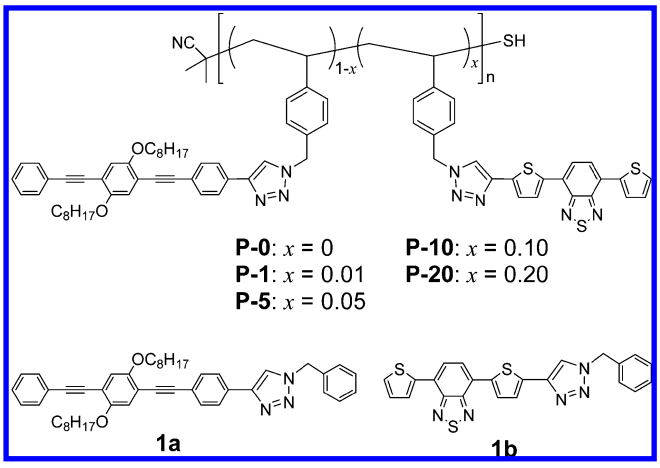



dx.doi.org/10.1021/jp411565p | J. Phys. Chem. B 2014, 118, 372−378

**Scheme 1. Preparation of Polychromophores (P-0 to P-20)**

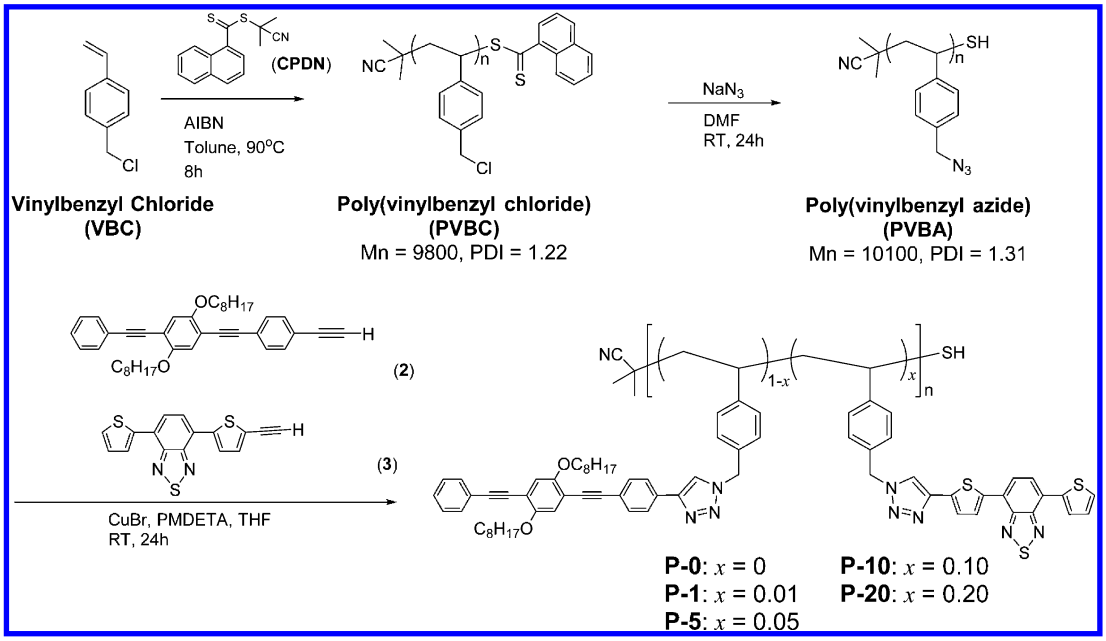


the synthesis of model compounds (**1a** and **1b**) and other small molecules are detailed in Supporting Information. Reversible addition−fragmentation transfer (RAFT) polymerization of 4-vinylbenzyl chloride afforded a polystyrene backbone with chloromethyl functionality (poly(4-vinylbenzyl chloride), PVBC), which has a molecular weight ($M_n$) of 9800 (DP ∼ 60) and a low polydispersity index (PDI) of 1.22. The "clickable" polystyrene backbone, poly(4-vinylbenzyl azide) (PVBA, $M_n$ ∼ 10,100 and PDI ∼ 1.31) was then obtained by chloride to azide $S_N2$ reaction. The five polychromophores were obtained by grafting the two chromophores with terminal alkyne (**2** and **3**) onto PVBA precursor via Cu(I)-catalyzed azide−alkyne "click" reaction.[18] All five polychromophores were derived from the same PVBA precursor so they all have the same chain length and degree of polymerization (DP ∼ 60). The chromophore loading ratio (***x***) was controlled by the ratio of the monomers used in the "click" reaction feed; the values of ***x*** in the polymer samples were confirmed by UV−visible absorption. While it was possible to construct an OPE (donor)-only polymer (**P-0**), the TBT (acceptor)-only polymer could not be studied because it is insoluble.

The synthetic transformation from PVBC to the poly chromophores was monitored by $^1$H NMR and GPC (Figure 1a and 1b). During the $S_N2$ reaction (from PVBC to PVBA), the peak at 4.52 ppm which is assigned to chloromethyl protons completely disappeared and the peak at 4.27 ppm (assigned to azidomethyl protons arises), indicating that chloride in each repeat unit of PVBC was completely substituted by azide. The complete "click" grafting was evidenced by the peak shift from 4.27 ppm (azidomethyl protons) shifts to 5.30 ppm (triazolemethylene protons). In addition, a peak at 3.98 ppm appeared after "click" reaction, which belongs to protons in oxymethylene groups in OPE side groups. The GPC traces showed there is no branching or cross-linking during the $S_N2$ and "click" grafting postpolymerization modification. All **P-*x*** polymers had significant molecular weight increase compared to PVBA precursor but still retaining low PDI values.

**Optical Properties of the Polychromophores.** To provide reference data for the isolated chromophores, OPE

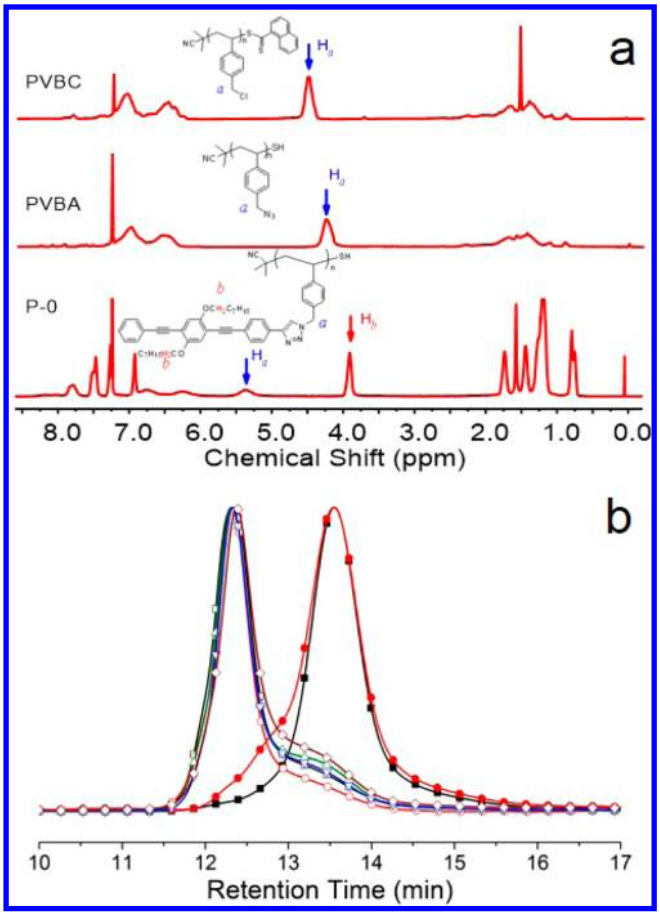


**Figure 1.** (a) $^1$H NMR spectra of PVBC, PVBA, and **P-0**. The detailed NMR spectra of **P-1** to **P-20** are shown in Figure S1 of Supporting Information. (b) GPC traces of polymers, **P-0** (black hollow squares, $M_n$ = 29200, PDI = 1.23), **P-1** (red hollow circle, $M_n$ = 29200, PDI = 1.17), **P-5** (green hollow triangle, $M_n$ = 28700, PDI = 1.23), **P-10** (blue hollow inverted triangle, $M_n$ = 28100, PDI = 1.23), **P-20** (brown hollow diamond, $M_n$ = 26800, PDI = 1.23), PVBC (black solid square, $M_n$ = 9800, PDI = 1.22), and PVBA (red solid circle, $M_n$ = 10100, PDI = 1.31).


dx.doi.org/10.1021/jp411565p | J. Phys. Chem. B 2014, 118, 372−378

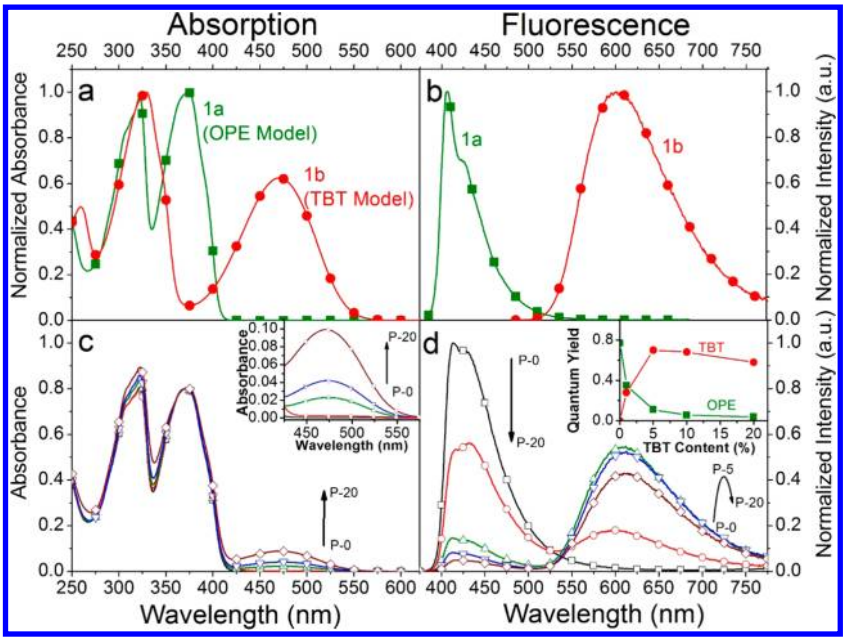


**Figure 2.** (a) Steady-state absorption of model compounds **1a** (green solid squares, $\varepsilon_{375\ nm}$ = 58000 $M^{-1}$ $cm^{-1}$) and **1b** (red solid circles, $\varepsilon_{470\ nm}$ = 24000 $M^{-1}$ $cm^{-1}$). (b) Fluorescence emission of OPE ($\phi_{fl}$ = 1.0) and TBT ($\phi_{fl}$ = 0.75). (c) Steady-state absorption of polymers, **P-0** (black hollow squares), **P-1** (red hollow circles), **P-5** (green hollow triangles), **P-10** (blue hollow inverted triangles), and **P-20** (brown hollow diamonds). All polymers were dissolved in THF. The inset is the absorption from TBT motif for the five polymers. (d) Fluorescence spectra of polymers, **P-0** to **P-20**. All polymers were dissolved in THF with an OD = 0.8 at 370 nm. The inset shows quantum yields of OPE emission (green solid squares, 370 to 510 nm) and TBT emission (red solid circles, 510 to 775 nm) for the five polymers. For panels c and d, arrows show directions of change with increasing TBT content in the copolymers.

**Table 1. Photophysical Characteristics of Polychromophores (P-0 to P-20)**

| Polymer | TBT Content[a] /% | Emission Lifetime at 420 nm[b] /ns | Emission Lifetime at 600 nm[b] /ns | Fluorescence Quantum Yield[c] | | | Energy Transfer Efficiency[d] /% | Model time constants and amplitudes at 665nm[e] | | |
|---|---|---|---|---|---|---|---|---|---|---|
| | | | | OPE Emission (375 – 525 nm) | TBT Emission (525 – 775 nm) | Overall (375-775 nm) | | $\tau_1$ /ps (A1) | $\tau_2$ /ps (A2) | $\tau_3$/ps (A3) |
| **P-0** | 0 | 2.63 (0.28)<br>1.00 (0.72) | - (-) | 0.77 | - | 0.77 | 0 | -<br>(-) | 44.9 ± 4.7<br>(0.20 ± 0.01) | 1148 ± 35<br>(0.80 ± 0.01) |
| **P-1** | 0.97 | 2.02 (0.31)<br>0.58 (0.69) | 10.60 (0.9)<br>3.04 (0.1) | 0.35 | 0.28 | 0.63 | 54.5 | 2.6 ± 0.7<br>(0.07 ± 0.01) | 56.8 ± 4.6<br>(0.31 ± .01) | 960 ± 34<br>(0.61 ± 0.01) |
| **P-5** | 5.4 | 2.04 (0.24)<br>0.35 (0.76) | 10.10 (1.0) | 0.11 | 0.7 | 0.81 | 85.7 | 3.4 ± 0.5<br>(0.23 ± 0.02) | 44.8 ± 3.7<br>(0.44 ± 0.02) | 1240 ± 112<br>(0.33 ± 0.01) |
| **P-10** | 11.0 | 1.90 (0.24)<br>0.36 (0.76) | 9.67 (1.0) | 0.056 | 0.68 | 0.74 | 92.7 | 2.1 ± 0.2<br>(0.26 ± 0.01) | 27.7 ± 1.5<br>(0.43 ± 0.01) | 1160 ± 66<br>(0.30 ± 0.01) |
| **P-20** | 20.0 | 1.78 (0.29)<br>0.36 (0.71) | 8.94 (1.0) | 0.039 | 0.58 | 0.62 | 94.9 | 2.0 ± 0.1<br>(0.38 ± 0.01) | 26.1 ± 2.1<br>(0.33 ± 0.01) | 1465 ± 110<br>(0.29 ± 0.01) |

[a]TBT content determined by UV–vis absorption. The ratio of absorbance of **P-*x*** polymers at 370 and 470 nm follows the equation $I_{(370\ nm,\ P\text{-}x)}/I_{(470\ nm,\ P\text{-}x)}=[(1-x)\varepsilon_{(370\ nm,\ 1a)}+x\,\varepsilon_{(370\ nm,\ 1b)}]/[x\varepsilon_{(470\ nm,\ 1b)}]$, in which $\varepsilon_{(370\ nm,\ 1a)}$ = 58000 $M^{-1}$ $cm^{-1}$, $\varepsilon_{(370\ nm,\ 1b)}$ = 2640 $M^{-1}$ $cm^{-1}$, and $\varepsilon_{(470\ nm,\ 1b)}$ = 24000 $M^{-1}$ $cm^{-1}$. [b]Emission lifetime measured by time-correlated single photon counting (TCSPC). [c]With anthracene as quantum yield standard, $\phi$ = 0.27 in ethanol at room temperature. [d]Energy transfer efficiencies ($\eta$) were calculated as $\eta = 1 - \phi(\text{OPE})/\phi(\textbf{P-0})$, in which $\phi$(**P-0**) was the fluorescence quantum yield of donor-only polymer **P-0**, and $\phi$(OPE) is OPE emission quantum yields of copolymers. [e]Measured from single wavelength transient absorption kinetics at $\lambda$ = 665 nm.

and TBT model compounds **1a** and **1b** (Chart 1) were studied, and their absorption and fluorescence spectra are shown in Figure 2, panels a and b. Table 1 provides a listing of photophysical parameters. OPE oligomer **1a** features two near-UV absorption bands (322 and 370 nm) and a single fluorescence band (407 nm) with a quantum yield of unity, $\phi_{fl}$ ~1.0.


dx.doi.org/10.1021/jp411565p | J. Phys. Chem. B 2014, 118, 372–378

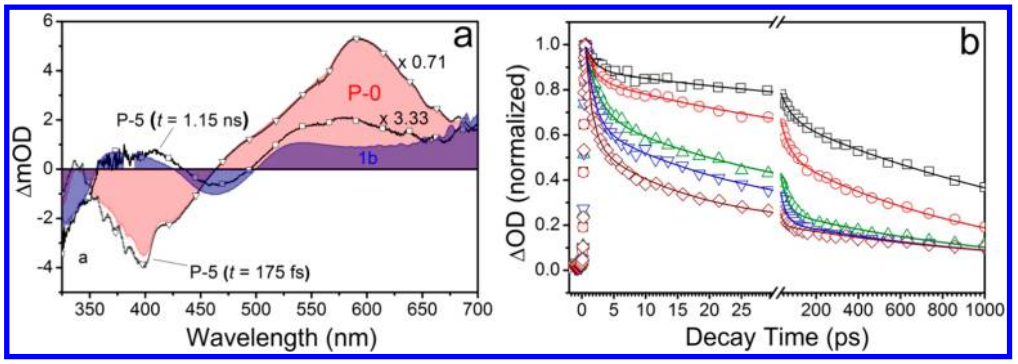


**Figure 3.** (a) Transient absorption spectra showing early time ($t$ = 175 fs) comparison between **P-5** (hollow triangles) and the pure donor polymer **P-0** (red filled). Also shown are transient spectra at $t$ = 1.15 ns comparing **P-5** (hollow squares) with the TBT acceptor moiety (blue filled). (b) Transient kinetics from $\lambda$ = 665 nm for the five polymers, **P-0** (black hollow squares), **P-1** (red hollow circles), **P-5** (green hollow triangles), **P-10** (blue hollow inverted triangles), and **P-20** (brown hollow diamonds).

The TBT oligomer **1b** exhibits a near-UV absorption band at 330 nm and a visible band at 470 nm. The fluorescence band from **1b** has a maximum at $\lambda \sim 600$ nm, with $\phi_{fl} \sim 0.75$.

The absorption spectra of the polychromophores are shown in Figure 2, panel c. The donor-only polymer, **P-0**, has essentially the same spectrum as that of OPE model compound **1a**, with bands in the near-UV at 322 and 370 nm. The spectra of **P-1** to **P-20** are dominated by the OPE-based transitions (especially at 370 nm); however, they show increasing TBT character as the loading of the lower energy chromophores in the click grafting is increased as evidenced by the appearance of visible transition at 470 nm (Figure 2c, inset). This feature allows straightforward determination of the TBT loading in the copolymer from the ratio of the absorbance at 370 and 470 nm (Table 1). Taken together, the absorption data for the model compounds and polymers allow several conclusions. First, the fractional loading of OPE and TBT units in the polymers closely corresponds to the stoichiometry used in the feed for the click reactions. Second, the absorption at 370 nm is due almost exclusively to the OPE (donor), making it possible to selectively excite this chromophore. Finally, the polymer spectra are accurately simulated as a linear combination of the spectra of the OPE and TBT chromophores (Figure S2 in Supporting Information), indicating that there is not a strong ground-state interaction among the individual units in the polymers.

Figure 2, panel d, shows the fluorescence spectra of all five polymers. In this experiment the concentration of the polymer solutions was adjusted such that the absorption at the 370 nm excitation wavelength was identical ($\Delta$OD = 0.8). The fluorescence of the OPE (donor)-only polymer **P-0** ($\lambda$ = 413 nm) appears as a single band which is slightly red-shifted and broadened compared to that of the OPE model **1a**; this result suggests that there is some interchromophore interaction in the singlet excited state. Interestingly, in **P-1**, the emission from the OPE chromophore at 413 nm is quenched ~40% relative to the intensity of **P-0**, and fluorescence from the TBT units at 600 nm is evident, indicating that OPE to TBT energy transfer is efficient. Calculations based on the fluorescence quantum yields of the donor and acceptor reveal that the energy transfer efficiency in **P-1** is ~55%. In **P-5**, the OPE emission is quenched to a greater extent, and the energy transfer efficiency from OPE to TBT approaches 85%. This trend continues through the series as seen in Figure 2d (inset) where the quantum yields of OPE and TBT fluorescence in the **P-*x*** series is plotted (see Table 1 for energy transfer efficiencies). Note that the OPE emission yield decreases sharply from **P-0** to **P-5**, followed by a more gradual decline from **P-10** to **P-20**. By contrast, the TBT emission yield increases sharply from **P-0** to **P-5**; however, it then decreases slightly from **P-5** to **P-20**. The latter trend is likely due to self-quenching of the TBT chromophore as its concentration in the polymers increases, possibly due to interchromophore charge transfer interaction between TBT units. The self-quenching mechanism is supported by the fact that the lifetime of the TBT fluorescence also decreases from **P-5** to **P-20** (Table 1). Excitation spectra for the **P-*x*** series collected while monitoring emission at 610 nm clearly show that the TBT emission results from excitation of the OPE chromophores (Figure S3 in Supporting Information).

**Ultrafast Transient Absorption Spectroscopy.** Ultrafast transient absorption experiments were carried out on the polychromophores to characterize the dynamics of the intrapolymer energy transfer process. Figure 3 compares the ultrafast transient absorption of the donor–acceptor copolymers (**P-1** to **P-20**) with those of the donor-only polymer (**P-0**) and the TBT acceptor unit as modeled by **1b**. The transient spectrum of **P-0** (Figure 3a, red filled) shows a negative feature (bleach) at 400 nm that results from a combination of ground-state bleach and stimulated OPE emission, as well as an intense excited-state absorption centered near 600 nm. The single wavelength kinetic trace of **P-0** (Figure 3b, black hollow squares) measured at $\lambda$ = 665 nm shows a biphasic decay. The minor component (0.20) has a 50 ps lifetime and is attributed to relaxation dynamics within the singlet excited state, likely due to planarization of the OPE unit.[30] This decay is accompanied by a slight blue shift of the excited-state absorption. The major decay component (0.80) has a 1.2 ns lifetime and is consistent with the excited-state lifetime measured from the fluorescence decay kinetics.[31]

Examination of the transient absorption of **P-5** reveals the importance of energy transfer to the excited-state dynamics when both OPE donor and TBT acceptor moieties are present on a single chain. Figure 3a shows the transient absorption spectrum of the **P-5** donor–acceptor copolymer at 175 fs (hollow triangles). The spectrum is nearly identical to that of the OPE donor-only polymer, **P-0** (red filled), indicating that photoexcitation at 388 nm predominantly creates OPE excited states (OPE*). However, by 1.1 ns following excitation the transient spectrum of **P-5** (hollow squares) has evolved, now containing absorption and bleach features that are very similar to those of the excited TBT chromophore (TBT*, compare with transient spectrum of TBT model **1b**, blue filled). These transient absorption results are in accord with the fluorescence spectra, confirming the occurrence of efficient intrachain OPE to TBT energy transfer.


dx.doi.org/10.1021/jp411565p | J. Phys. Chem. B 2014, 118, 372–378

The dynamics of energy transfer can in principle be followed either through the disappearance of OPE* (i.e., donor decay) or appearance of TBT* (acceptor rise). However, monitoring the appearance of TBT* via its ground-state bleach at $\lambda = 470$ nm is problematic due to the stimulated emission from OPE* in this spectral region. We have instead focused our analysis on the decay of OPE* absorption at 665 nm, where the OPE* stimulated emission and TBT* contributions are minimized.[32] Thus, the single wavelength kinetic trace of **P-5** (Figure 3b, green hollow triangles) exhibits decay dynamicss much faster than that of donor-only **P-0**. The accelerated decay is primarily caused by an additional fast component ($\tau_1 \approx 3.4$ ps), which is assigned to quenching of OPE* excitons formed on a chain in close spatial proximity to a TBT acceptor unit and that undergo direct energy transfer to the acceptor. In addition to this fastest component, there is also an intermediate component ($\tau_2 \approx 26$ ps) likely reflecting two processes: relaxation of the initially formed excited state that is observed in the donor-only polymer,[30] as well as multistep energy transfer in which the excited state first has to migrate through a random walk, site-to-site hopping process to a position along the chain that is in close proximity to an acceptor. The overall time scale for this latter process will depend on the OPE−OPE hopping rate ($k_{hop}$), the number of hops needed to reach the trap, as well as the OPE−TBT energy transfer rate ($k_{EnT}$).

Across the polymer series, a trend of faster OPE* decay is observed as loading of the TBT acceptor units increases. The additional fast ($\tau_1$) decay component as well as greater contribution from intermediate rate processes (relative to that seen in **P-0**) is found for each of the other copolymers in the series. Time constants and normalized amplitudes recovered from the triexponential modeling of the five **P-*x*** polymers are summarized in Table 1. In general, with increased TBT content, the amplitude of the ∼3 ps component increases at the expense of that for the intermediate component. Increasing the loading of the TBT acceptor chromophores in the copolymer has two effects. First, the probability of photoexcitation producing excited states within the quenching radius of an acceptor increases. Second, for those excitons created far from an acceptor, the number of steps necessary to migrate near enough for quenching to occur decreases. Both of these effects will result in qualitatively faster quenching of the excited state, a result which can be seen by comparing the kinetics at 665 nm for the polymer series. In particular, as the loading increases from 1% to 20%, the amplitude of the fast component increases from 0.07 to 0.38 with little change in the time constant itself, consistent with the direct OPE* to TBT energy transfer assignment (Table 1). Closer inspection shows that the amplitude rolls over at higher TBT fractions, reflecting the qualitative expectation that the probability of finding at least one TBT nearest neighbor will level off as the TBT content increases. While this is qualitatively consistent with direct energy transfer, quantitative analysis proved to be problematic due to the contribution of TBT* to the transient at the probe wavelength. Furthermore, the time constant associated with the intermediate processes (25−50 ps) trends downward as loading increases, reflecting the shorter amount of time necessary for an excited state to migrate to the TBT trap.

**Molecular Dynamics Simulations.** To examine the relationship between energy transfer and polymer structure, we performed molecular dynamics (MD) simulations of a 30-unit subsection of the **P-0**, **P-5**, **P-10**, and **P-20** polymers with explicit THF solvent. On average, the nearest neighbor chromophore distance (regardless of whether it was an OPE−OPE pair or an OPE−TBT pair) was found to be 0.99 ± 0.23 nm. This distance used in the Förster expression predicts rates that are greater than those observed experimentally: an OPE/OPE hopping rate of $k_{hop} = 0.53 \times 10^{12}$ s$^{-1}$ and an OPE/TBT energy transfer rate of $k_{EnT} = 4.8 \times 10^{12}$ s$^{-1}$. However, given the nature of energy transfer in this polymer, an overestimation of the energy transfer rate by standard point-dipole Förster theory may be expected. The polystyrene backbone is not electronically coupled to either donor or acceptor, so energy transfer will proceed via through-space interactions of donor and acceptor chromophores that are oriented roughly cofacially. In this case, Förster theory tends to overestimate the energy transfer rate unless more elaborate methods are used for the Coulomb interaction.[33,34] Consequently, while quantitative comparison with experimentally determined rates is invalid, the average interchromophore distance calculated from MD simulations is well within the Förster radii calculated from spectral overlap and the OPE quantum yield for both energy transfer ($R_0 = 4.11$ nm) and hopping processes ($R_0 = 2.72$ nm). This suggests that both direct ($\tau_1$) and hopping ($\tau_2$) routes are efficient mechanisms of energy migration and transfer. As a result, the polymer motif serves to efficiently couple donor and acceptor chromophores, creating a network that quickly shuttles energy on the nanoscale and may be a promising model for light-harvesting applications. This concept can be implemented by application of synthetic methods similar to those used in the present work to construct acceptor-end functional or donor−acceptor diblock architectures which could utilize the efficient energy transfer in a vectorial sense.

## CONCLUSION

In summary, we have examined energy transport in a light-harvesting polymer consisting of ∼60 OPE chromophores. Photoexcitation of OPE sites gives rise to site-to-site energy transfer and ultimately sensitization of a trap site (TBT) doped into the polymer at low concentration, on the picosecond time scale and with remarkably high efficiency. The energy transfer process proceeds via ultrafast neighborhood OPE-TBT quenching in 2−4 ps and OPE-OPE energy hopping in 25−50 ps.

## ASSOCIATED CONTENT

### Supporting Information

Detailed synthesis and experimental procedures, monomer and polymer characterization data, and additional spectroscopic data. This material is available free of charge via the Internet at http://pubs.acs.org.

## AUTHOR INFORMATION

### Corresponding Authors

*E-mail: kschanze@chem.ufl.edu.
*E-mail: john_papanikolas@unc.edu.

### Author Contributions

[§]These authors contributed equally.

### Notes

The authors declare no competing financial interests.

## ACKNOWLEDGMENTS

This material is based solely on work supported as part of the UNC EFRC: Center for Solar Fuels, an Energy Frontier Research Center funded by the U.S. Department of Energy, Office of Science, Office of Basic Energy Sciences under Award Number DE-SC0001011.

## REFERENCES


(1) Webber, S. E. Photon-Harvesting Polymers. *Chem. Rev.* **1990**, *90*, 1469−1482.

(2) Fox, M. A.; Jones, W. E.; Watkins, D. M. Light-Harvesting Polymer Systems. *Chem. Eng. News* **1993**, *71*, 38−48.

(3) Adronov, A.; Gilat, S. L.; Fréchet, J. M. J.; Ohta, K.; Neuwahl, F. V. R.; Fleming, G. R. Light Harvesting and Energy Transfer in Laser−Dye-Labeled Poly(aryl ether) Dendrimers. *J. Am. Chem. Soc.* **2000**, *122*, 1175−1185.

(4) Wells, N. P.; Boudouris, B. W.; Hillmyer, M. A.; Blank, D. A. Intramolecular Exciton Relaxation and Migration Dynamics in Poly(3-hexylthiophene). *J. Phys. Chem. C* **2007**, *111*, 15404−15414.

(5) Barford, W.; Lidzey, D. G.; Makhov, D. V.; Meijer, A. J. H. Exciton localization in disordered poly(3-hexylthiophene). *J. Chem. Phys.* **2010**, *133*, 044504.

(6) Busby, E.; Carroll, E. C.; Chinn, E. M.; Chang, L.; Moulé, A. J.; Larsen, D. S. Excited-State Self-Trapping and Ground-State Relaxation Dynamics in Poly(3-hexylthiophene) Resolved with Broadband Pump−Dump−Probe Spectroscopy. *J. Phys. Chem. Lett.* **2011**, *2*, 2764−2769.

(7) Lewis, A. J.; Ruseckas, A.; Gaudin, O. P. M.; Webster, G. R.; Burn, P. L.; Samuel, I. D. W. Singlet Exciton Diffusion in MEH-PPV Films Studied by Exciton−Exciton Annihilation. *Org. Electron.* **2006**, *7*, 452−456.

(8) Markov, D. E.; Amsterdam, E.; Blom, P. W. M.; Sieval, A. B.; Hummelen, J. C. Accurate Measurement of the Exciton Diffusion Length in a Conjugated Polymer Using a Heterostructure with a Side-Chain Cross-Linked Fullerene Layer. *J. Phys. Chem. A* **2005**, *109*, 5266−5274.

(9) Mikhnenko, O. V.; Cordella, F.; Sieval, A. B.; Hummelen, J. C.; Blom, P. W. M.; Loi, M. A. Temperature Dependence of Exciton Diffusion in Conjugated Polymers. *J. Phys. Chem. B* **2008**, *112*, 11601−11604.

(10) Pensack, R. D.; Banyas, K. M.; Barbour, L. W.; Hegadorn, M.; Asbury, J. B. Ultrafast Vibrational Spectroscopy of Charge-Carrier Dynamics in Organic Photovoltaic Materials. *Phys. Chem. Chem. Phys.* **2009**, *11*, 2575−2591.

(11) Shaw, P. E.; Ruseckas, A.; Samuel, I. D. W. Exciton Diffusion Measurements in Poly(3-hexylthiophene). *Adv. Mater.* **2008**, *20*, 3516−3520.

(12) Wang, L.; Puodziukynaite, E.; Vary, R. P.; Grumstrup, E. M.; Walczak, R. M.; Zolotarskaya, O. Y.; Schanze, K. S.; Reynolds, J. R.; Papanikolas, J. M. Competition between Ultrafast Energy Flow and Electron Transfer in a Ru(II)-Loaded Polyfluorene Light-Harvesting Polymer. *J. Phys. Chem. Lett.* **2012**, *3*, 2453−2457.

(13) Fox, M. A. Polymeric and Supramolecular Arrays for Directional Energy and Electron Transport over Macroscopic Distances. *Acc. Chem. Res.* **1992**, *25*, 569−574.

(14) Fox, M. A. Photophysical Probes for Multiple-Redox and Multiple-Excited-State Interactions in Molecular Aggregates. *Acc. Chem. Res.* **2012**, *45*, 1875−1886.

(15) Friesen, D. A.; Kajita, T.; Danielson, E.; Meyer, T. J. Preparation and Photophysical Properties of Amide-Linked, Polypyridylruthenium-Derivatized Polystyrene. *Inorg. Chem.* **1998**, *37*, 2756−2762.

(16) Furuta, P. T.; Deng, L.; Garon, S.; Thompson, M. E.; Fréchet, J. M. J. Platinum-Functionalized Random Copolymers for Use in Solution-Processible, Efficient, Near-White Organic Light-Emitting Diodes. *J. Am. Chem. Soc.* **2004**, *126*, 15388−15389.

(17) Mei, J.; Aitken, B. S.; Graham, K. R.; Wagener, K. B.; Reynolds, J. R. Regioregular Electroactive Polyolefins with Precisely Sequenced $\pi$-Conjugated Chromophores. *Macromolecules* **2010**, *43*, 5909−5913.

(18) Sun, Y.; Chen, Z.; Puodziukynaite, E.; Jenkins, D. M.; Reynolds, J. R.; Schanze, K. S. Light Harvesting Arrays of Polypyridine Ruthenium-(II) Chromophores Prepared by Reversible Addition−Fragmentation Chain Transfer Polymerization. *Macromolecules* **2012**, *45*, 2632−2642.

(19) Watkins, D. M.; Fox, M. A. Rigid, Well-Defined Block Copolymers for Efficient Light Harvesting. *J. Am. Chem. Soc.* **1994**, *116*, 6441−6442.

(20) Adronov, A.; Fréchet, J. Light-Harvesting Dendrimers. *Chem. Commun.* **2000**, 1701−1710.

(21) Devadoss, C.; Bharathi, P.; Moore, J. S. Energy Transfer in Dendritic Macromolecules: Molecular Size Effects and the Role of an Energy Gradient. *J. Am. Chem. Soc.* **1996**, *118*, 9635−9644.

(22) Feng, F.; Lee, S. H.; Cho, S. W.; Kömürlü, S.; McCarley, T. D.; Roitberg, A.; Kleiman, V. D.; Schanze, K. S. Conjugated Polyelectrolyte Dendrimers: Aggregation, Photophysics, and Amplified Quenching. *Langmuir* **2012**, *28*, 16679−16691.

(23) Imahori, H. Giant Multiporphyrin Arrays as Artificial Light-Harvesting Antennas. *J. Phys. Chem. B* **2004**, *108*, 6130−6143.

(24) Jones, G., II; Rahman, M. A. Fluorescence Energy Transfer between Coumarin Laser Dyes Co-bound to Poly(methacrylic acid) in Water. *Chem. Phys. Lett.* **1992**, *200*, 241−250.

(25) Breul, A. M.; Schäfer, J.; Pavlov, G. M.; Teichler, A.; Höppener, S.; Weber, C.; Nowotny, J.; Blankenburg, L.; Popp, J.; Hager, M. D.; Dietzek, B.; Schubert, U. S. Synthesis and Characterization of Polymethacrylates Containing Conjugated Oligo(phenylene ethynylene)s as Side Chains. *J. Polym. Sci., Part A: Polym. Chem.* **2012**, *50*, 3192−3205.

(26) Schäfer, J.; Breul, A.; Birckner, E.; Hager, M. D.; Schubert, U. S.; Popp, J.; Dietzek, B. Fluorescence Study of Energy Transfer in PMMA Polymers with Pendant Oligo-Phenylene-Ethynylenes. *ChemPhysChem* **2013**, *14*, 170−178.

(27) Beljonne, D.; Pourtois, G.; Silva, C.; Hennebicq, E.; Herz, L. M.; Friend, R. H.; Scholes, G. D.; Setayesh, S.; Müllen, K.; Brédas, J. L. Interchain vs. Intrachain Energy Transfer in Acceptor-Capped Conjugated Polymers. *Proc. Natl. Acad. Sci. U.S.A.* **2002**, *99*, 10982−10987.

(28) Frisch, M. J. T. G. W.; Schlegel, H. B.; Scuseria, G. E.; Robb, M. A.; Cheeseman, J. R.; Montgomery, J. A., Jr.; Vreven, T.; Kudin, K. N.; Burant, J. C.; Millam, J. M.; Iyengar, S. S.; Tomasi, J.; Barone, V.; Mennucci, B.; Cossi, M.; Scalmani, G.; Rega, N.; Petersson, G. A.; Nakatsuji, H.; Hada, M.; Ehara, M.; Toyota, K.; Fukuda, R.; Hasegawa, J.; Ishida, M.; Nakajima, T.; Honda, Y.; Kitao, O.; Nakai, H.; Klene, M.; Li, X.; Knox, J. E.; Hratchian, H. P.; Cross, J. B.; Bakken, V.; Adamo, C.; Jaramillo, J.; Gomperts, R.; Stratmann, R. E.; Yazyev, O.; Austin, A. J.; Cammi, R.; Pomelli, C.; Ochterski, J. W.; Ayala, P. Y.; Morokuma, K.; Voth, G. A.; Salvador, P.; Dannenberg, J. J.; Zakrzewski, V. G.; Dapprich, S.; Daniels, A. D.; Strain, M. C.; Farkas, O.; Malick, D. K.; Rabuck, A. D.; Raghavachari, K.; Foresman, J. B.; Ortiz, J. V.; Cui, Q.; Baboul, A. G.; Clifford, S.; Cioslowski, J.; Stefanov, B. B.; Liu, G.; Liashenko, A.; Piskorz, P.; Komaromi, I.; Martin, R. L.; Fox, D. J.; Keith, T.; Al-Laham, M. A.; Peng, C. Y.; Nanayakkara, A.; Challacombe, M.; Gill, P. M. W.; Johnson, B.; Chen, W.; Wong, M. W.; Gonzalez, C.; Pople, J. A. *Gaussian 09, revision A.2*, Gaussian, Inc., Wallingford, CT, 2009.

(29) Rappe, A. K.; Casewit, C. J.; Colwell, K. S.; Goddard, W. A.; Skiff, W. M. UFF, a Full Periodic Table Force Field for Molecular Mechanics and Molecular Dynamics Simulations. *J. Am. Chem. Soc.* **1992**, *114*, 10024−10035.

(30) Sluch, M. I.; Godt, A.; Bunz, U. H. F.; Berg, M. A. Excited-State Dynamics of Oligo(*p*-phenyleneethynylene): Quadratic Coupling and Torsional Motions. *J. Am. Chem. Soc.* **2001**, *123*, 6447−6448.

(31) As the laser fluence is increased above 40 $\mu$J/cm$^2$, the excited-state absorption begins to exhibit intensity-dependent kinetics, presumably due to exciton−exciton annihilation events that occur when more than one excited state is created on each chain. The transient data reported here were collected at pulse energies below this threshold (25 $\mu$J/cm$^2$), thus avoiding these exciton−exciton processes.

(32) Global analysis of the transient absorption spectral-kinetic data affords similar results as single wavelength analysis.

(33) Wong, K. F.; Bagchi, B.; Rossky, P. J. Distance and Orientation Dependence of Excitation Transfer Rates in Conjugated Systems: Beyond the Förster Theory. *J. Phys. Chem. A* **2004**, *108*, 5752−5763.

(34) Khan, Y. R.; Dykstra, T. E.; Scholes, G. D. Exploring the Förster Limit in a Small FRET Pair. *Chem. Phys. Lett.* **2008**, *461*, 305−309.